*J. Fluid Mech.* (2006), *vol.* 554, *pp.* 47–66.  
doi:10.1017/S0022112006009189 Printed in the United Kingdom

# On the elasticity of an inertial liquid shock

By ANNE-LAURE BIANCE[1], FRÉDÉRIC CHEVY[1], CHRISTOPHE CLANET[2], GUILLAUME LAGUBEAU[2] AND DAVID QUÉRÉ[1]

[1]Laboratoire de Physique de la Matière Condensée, FRE 2844 du CNRS, Collège de France 75231 Paris Cedex 05, France

[2]Institut de Recherche sur les Phénomènes Hors Équilibre, UMR 6594 du CNRS BP 146, 13384 Marseille Cedex, France

(Received 26 September 2005 and in revised form 10 January 2006)

A drop of low viscosity hitting a solid may bounce, provided that the material is highly hydrophobic. As a model of such a situation, we consider here the case of a very hot solid. Then, as discovered by Leidenfrost, a thin layer of vapour sustains the drop, preventing any contact with the substrate. On hitting such a solid, a drop rebounds, and we discuss here the elasticity of the shock. Two very different cases are described: at a large velocity, the weaker the impact velocity, the weaker the elasticity; at a small velocity, a quasi-elastic regime is found. The boundary between the two domains is set by a Weber number, which compares the kinetic and surface energies of the drop, of order unity.

## 1. Introduction

In 1756, two hundred years before the foundation of the *Journal of Fluid Mechanics*, Johan Leidenfrost, a German physician from Duisburg, published a summary of his discoveries on the physics of drops (Leidenfrost 1756). He described in particular the remarkable behaviour of volatile liquids when deposited on substrates whose temperature is significantly higher than the liquid's boiling point (Gottfried, Lee & Bell 1966; Baumeister & Simon 1973). For water on copper or iron at a temperature of about 200 °C (or more), it is observed that drops are extremely mobile and quickly roll off the substrate if any slope is present. On a curved surface (such as the inside of a spoon, in order to keep the drop trapped), the liquid does not boil and remains for a very long time (typically a few minutes for millimetric drops), despite the high temperature of the substrate (Bell 1967).

Leidenfrost correctly interpreted these experiments. He understood that a vapour film forms between the drop and the substrate, allowing the liquid to levitate (Goldshtik, Khanin & Ligai 1985). Because of the absence of contact, bubble nucleation is inhibited (no boiling), and the existence of a cushion of air dramatically reduces the friction with the substrate. Since a gas is a good insulator, the heat transfer is not efficient in the film, so that there is a relatively slow evaporation for the liquid (Berenson 1961; Watchers, Bonn & Van Nouhuis 1966; Michiyoshi & Makino 1978; Zhang & Gogos 1991; Chandra & Avedisian 1994). By placing a candle behind the drop and looking through the base, Leidenfrost saw a sheet of light of thickness of about 100 μm (a hair's diameter), allowing him not only to prove the existence of the vapour film, but also to measure its (correct) typical thickness (Biance, Clanet & Quere, 2003).

The shape of the drops is also of interest. While large centimetric drops are flattened by gravity, small millimetric droplets are quasi-spherical, which was understood (by Young and Laplace) 50 years after Leidenfrost's observations to be a consequence of the cohesion of liquids: a drop has a surface energy proportional to its area, whose minimum corresponds to a spherical shape. The surface energy per unit area is called the surface tension and denoted as $\gamma$. For a Leidenfrost water drop, evaporation maintains the drop temperature at 100 °C, so that the surface tension is fixed at 58 mN m$^{-1}$ (this condition of constant temperature should limit Marangoni effects in the drop). This allows us to specify when gravity can be neglected: while the surface energy of a drop of size $R$ scales as $\gamma R^2$, its gravitational energy is proportional to $\rho g R^4$, where $\rho$ denotes the liquid density and $g$ denotes the acceleration due to gravity. Hence, gravity is negligible provided that the drop is smaller than the so-called capillary length, $\kappa^{-1} = (\gamma/\rho g)^{1/2}$. For water at 100 °C, $\kappa^{-1} = 2.5$ mm; for less cohesive liquids (such as light oils or liquid nitrogen), it can be as low as 1 mm.

Apart from these classical static properties, such non-adhesive Leidenfrost drops have a remarkable dynamic characteristics: if they impact a surface, they bounce, as solid spheres do (Richard & Quéré 2000; Karl & Frohn 2000). This does not happen for common liquid impacts; then, the kinetic energy is dissipated by viscosity as the drop spreads on its substrate (Rein 1993), in particular owing to the moving contact lines close to which viscous losses are enhanced. For Leidenfrost drops, there is no contact line, and the kinetic energy efficiently converts to surface energy (the drop deforms as it hits the solid) and then to kinetic energy again, allowing the system to behave as an elastic spring. This directly shows how the contact time of a bouncing drop scales with the different parameters (Richard, Clanet & Quéré 2002): the liquid surface tension $\gamma$ is the stiffness of this spring and $\rho R^3$ is its mass, so that the natural response time scales as $(\rho R^3/\gamma)^{1/2}$, of the order of a few milliseconds for a millimetric drop – a time negligible compared to the lifetime of the globule.

Here we discuss the elasticity of this kind of liquid shock. We shall see that unlike what happens for solid shocks, the elasticity is very sensitive to the impact velocity. It is found in particular that the shock is more elastic when the impact speed is small. In the limit of very small velocities, the use of Leidenfrost drops leads to a regime of quasi-elastic rebounds. For larger velocities, the shock can be much less elastic; in addition, elasticity is lost above a critical radius (whatever the impact velocity), for which the weight dominates the surface effects. These series of experiments are interpreted using a minimal model.

## 2. Characteristics of a liquid impact

Figure 1 shows a typical sequence of events, observed as a water drop hits a silicon plate whose temperature (300 °C) is much larger than the boiling point of water. Here, the drop has a radius $R = 1$ mm, and it is released from a height $H = 3.2$ cm, so that the impact speed $V = \sqrt{2gH}$ is about 0.8 m s$^{-1}$. The pictures are taken with a high-speed camera (1000 frames per second), using back-lighting to improve the contrast.

As it impacts the solid, the drop deforms: it first spreads until it transiently forms a kind of non-wetting puddle, as it reaches its maximum extension. Then, it retracts and elongates in the vertical direction: the globule is highly deformed at take off (after a 'contact' time of 11 ms, in figure 1). As a consequence, it strongly vibrates as it rises; then, it reaches its maximum height, whose position can be measured. We deduce from such sequences the restitution coefficient $e = V'/V$ of the shock, defined

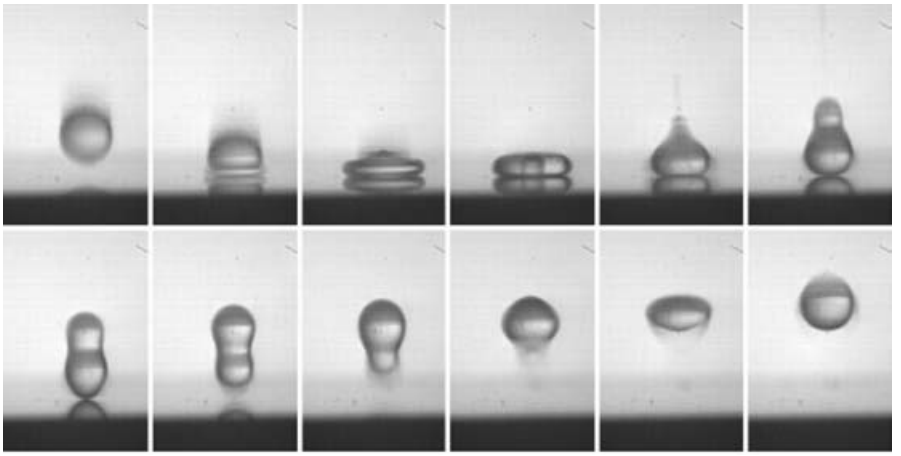

FIGURE 1. Rebound of a millimetric water drop hitting a steel plate heated at 300 °C. The time interval between two pictures is 1.8 ms. The drop radius is 1 mm, and the impact velocity is 80 cm s$^{-1}$. The corresponding Weber number (equation (1)) is about 10, meaning that large deformations are observed during the impact, leading to strong oscillations.

as the ratio between the velocities of the centre of mass after and before impact. In the example in figure 1, $e$ is 0.6, showing a modest elasticity (the final height of the drop is only 36 % of that from which it was released).

The contact time $\tau$ is defined as the interval between the moment when the drop reaches the plate and that when it leaves it. Measurements of $\tau$ are shown in figure 2 as a function of the impact velocity (for a fixed drop radius $R = 1.06$ mm), and as a function of drop radius (for a fixed impact velocity of 0.7 m s$^{-1}$). The results are very close to those observed for drops bouncing off super-hydrophobic substrates (Richard *et al.* 2002). On the one hand, the contact time is almost independent of the impact speed; it decreases very slightly as the speed increases, which might be related to the nonlinear regime of oscillation for strong deformations. On the other hand, the contact time rapidly increases with the drop size, as $R^{3/2}$ (shown with line). As the solid noted in the introduction, the contact time should be of the order of the oscillation time. This quantity was calculated by Rayleigh, for a drop freely oscillating in air (Rayleigh 1879). For the simplest (quadrupolar) mode of oscillation, this time is $\pi(\rho R^3/2\gamma)^{1/2}$, which exhibits the different scalings observed in figure 2. However, the numerical coefficient is slightly different: the Rayleigh coefficient $\pi/\sqrt{2}$ is about 2.2, while we deduce from the experiments a coefficient of $2.65 \pm 0.10$. Courty, Lagubeau & Tixier (2006) recently showed that the period of oscillation of a non-wetting drop is increased by the presence of a plate below, compared to a free drop. This might explain the slight disagreement found in the coefficient.

We also noted the existence of a well-defined state of maximal extension. We denote the radius of this transient puddle as $R_M$, and its thickness as $\delta$. We shall first consider the strong-deformation regime ($R_M \gg \delta$), which will occur if the kinetic energy of the impacting drop is much larger than its surface energy. The Weber number *We* compares these two energies:

$$We = \frac{\rho V^2 R}{\gamma}. \tag{1}$$

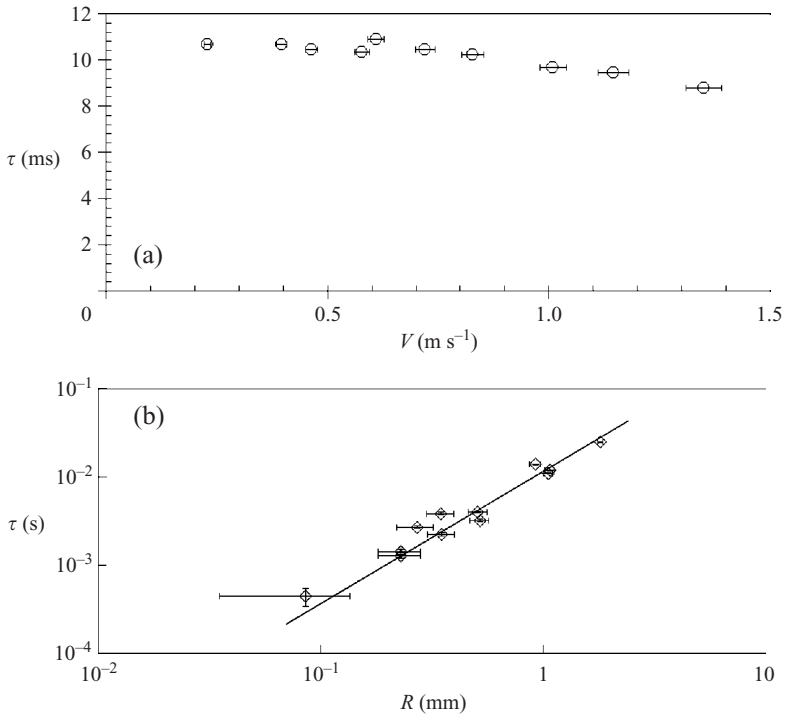


FIGURE 2. Contact time $\tau$ of a drop bouncing on plate heated at 280 °C. (*a*) $\tau$ is plotted as a function of the impact velocity $V$ (for a fixed drop radius $R = 1.06$ mm), and found to be quite insensitive to $V$ (multiplying $V$ by a factor of about 7 makes $\tau$ decrease by only 15 %). (*b*) $\tau$ is observed (in a log-log plot) to increase rapidly with the drop radius $R$, as $R^{3/2}$ (solid line). Writing $\tau = \alpha\ (\rho R^3/\gamma)^{1/2}$, we deduce from the fit a numerical coefficient $\alpha = 2.65 \pm 0.20$.

A strong deformation at impact corresponds to *We* larger than unity. The maximum radius should generally be a function of the Weber number. We could assume that the shock simply converts the kinetic energy (of the order of $\rho R^3 V^2$) to surface energy (of the order of $\gamma R_M^2$ in the limit considered here), which would yield (Chandra & Avedisian 1991):

$$R_M \sim R We^{1/2}. \tag{2}$$

But energy conservation is never straightforward in this kind of system, in particular because of the existence of internal flows during the contact time. We instead propose that the drop, as it hits the solid, is subjected to an acceleration which scales as $V^2/R$, since the velocity decreases from $V$ to 0 over a distance of about $R$ (Clanet *et al.* 2004). This acceleration is typically $100\,g$, in impact experiments, so that the drop will be (transiently) flattened, in this reinforced gravity field. The thickness $\delta$ of a non-wetting gravity puddle is proportional to a rescaled capillary length $\kappa^{-1} = (\gamma/\rho g)^{1/2}$, where $g$ must be replaced by $V^2/R$. Together with the volume conservation ($R^3 \sim \delta R_M^2$), this yields an extension:

$$R_M \sim R We^{1/4}. \tag{3}$$

This scaling appears to be different from the one arising from energy conservation: in the limit of large *We*, the drop is expected to be more contracted than predicted by (2), by a factor of $We^{1/4}$ (1.8 to 3.2, for *We* between 10 and 100). Of course, this

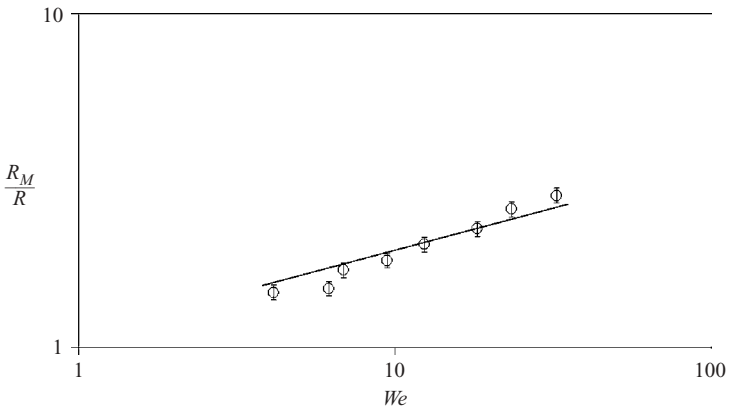


FIGURE 3. Maximum radius $R_M$ of a water drop impacting a plate heated at $T = 280\,^{\circ}\mathrm{C}$, as a function of the Weber number $We$ characterizing the shock and defined by equation (1). Drops radius is $R = 1.02\,\mathrm{mm}$, and the Weber number is varied by changing the impact velocity. The diagram has logarithmic scales, and the line shows the slope 0.25 – suggested by equation (3). Writing $R_M = \alpha We^{1/4}$, we deduce from the fit a numerical coefficient $\alpha = 1.1 \pm 0.1$.

description can only hold provided that the drop size $R$ is larger than the 'dynamic' capillary length $(\gamma R/\rho V^2)^{1/2}$ (only these drops will be flattened), so that again $We \gg 1$.

Figure 3 shows that the extension observed for the drop (and obtained owing to the variation of the impact velocity) follows a behaviour compatible with the scaling proposed in equation (3) (the exponent deduced from figure 3 is $0.30 \pm 0.05$). It is useful to define the maximum extension of the drop, because it defines the state from which the drop will retract and take off.

## 3. Elasticity of the shock: observations

We focus here on the elasticity of the shock. Our experiments consisted of filming rebounds for various liquids (water, ethanol, acetone, and liquid nitrogen), different drop radii $R$ (between 0.8 mm and 2 mm) and impact velocities $V$ (between $0.02\,\mathrm{m\,s^{-1}}$ and $1\,\mathrm{m\,s^{-1}}$). The case of larger drops (of size approaching the capillary length $\kappa^{-1}$) will be discussed separately (see § 4.2, and in particular figure 8). The plates were systematically at a 'high' temperature, that is, more than 100 °C above the boiling point of the liquid. Before impact, the drop is spherical and we extracted from the movies the position of the bottom of the drop. The impact velocities were varied by using different release heights, and the drop radii were changed using various hypodermic needles. The take-off speed $V'$ was deduced from the time $t$ at which the drop touched the solid again – during the flight, the drop is subject only to gravity, so that we simply have $V' = gt/2$.

We display in figure 4($a$) the variation of the restitution coefficient $e = V'/V$, as a function of the Weber number $We$ (defined in (1)). It is first observed that all the data collapse onto the same curve, showing that the Weber number is indeed the parameter which governs the shock elasticity. At low Weber number, $e$ is close to unity: the shock is quasi-elastic. At large $We$, the elasticity abruptly drops, to reach values as low as 0.2 for $We$ of about 30 (meaning that the drop rises after the shock to a height which is only 4 % of the initial height). This is our main finding: unlike solid shocks, the elasticity of liquid shocks (which imply strong deformations of the whole globule of matter) is extremely sensitive to the impact speed. Displaying the

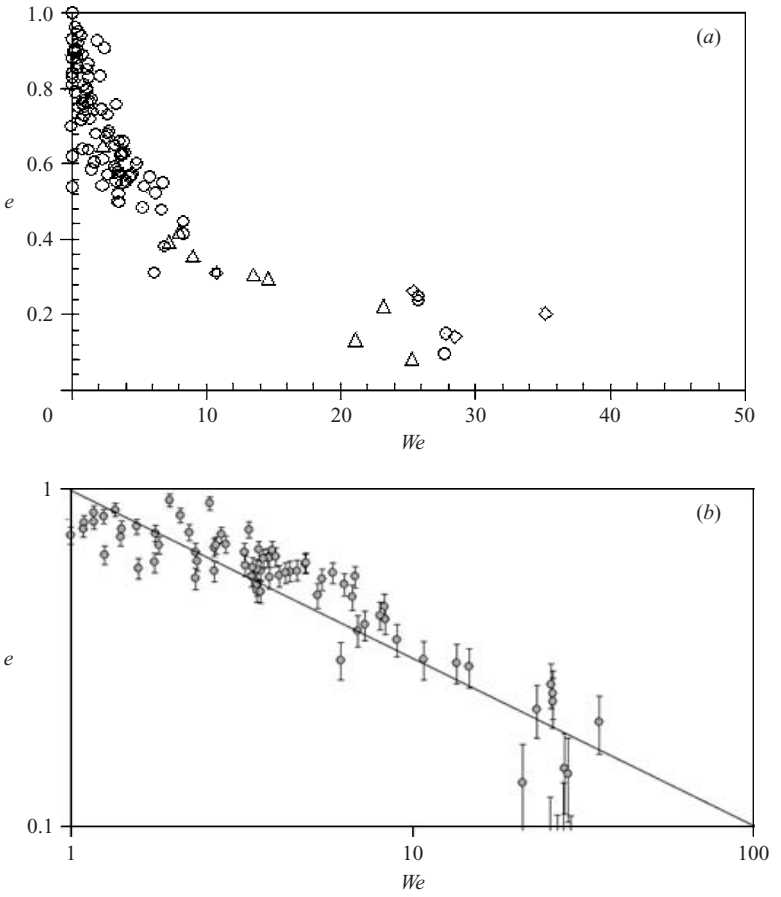


FIGURE 4. Restitution coefficient $e$ for Leidenfrost drops (○, water; △, acetone; ◇, ethanol; -, nitrogen) bouncing on plates at temperature much larger than the boiling point of the liquid. The drop radii vary between 0.8 and 2 mm, and the impact velocities between 0.02 and 1 m s$^{-1}$. (*a*) It is found that the data collapse on a single curve, if they are plotted as a function of the Weber number $We$ defined in (1). The elasticity strongly decreases with $We$. (*b*) If the same data are displayed in a log-log plot, $e$ is observed to decrease as $We^{-1/2}$ drawn with a line. Writing $e = \alpha We^{-1/2}$, we find from the fit a numerical coefficient $\alpha = 1.0 \pm 0.1$.

function $e(We)$ in a log-log plot (figure 4*b*) shows that the data for $We > 1$ can be described by the scaling $e \sim We^{-1/2}$.

These behaviours differ from what can be observed for drops impacting a super-hydrophobic surface (that is, a micro-textured hydrophobic surface on which contact angles are typically of the order of 160°). Then, as seen in figure 5, a strong decrease of the elasticity (compatible with a variation of $e$ as $1/V$) is also observed for 'large' impact velocities (corresponding, again, to large $We$). However, drops are found to stick to the substrate ($e = 0$) for moderate impact velocities ($V < 10$ cm s$^{-1}$). This can be interpreted as the result of the existence of a small adhesion force in this case: the kinetic energy of the drop becomes too low, so that pinning of the line on the surface textures allows the drop to remain stuck. This implies that smaller drops (of larger ratio surface/volume) will stick more easily than large ones, which was indeed observed (Richard 2000). As a consequence, the elasticity is maximum for some intermediate velocity, for which the restitution coefficient can (in this case) be

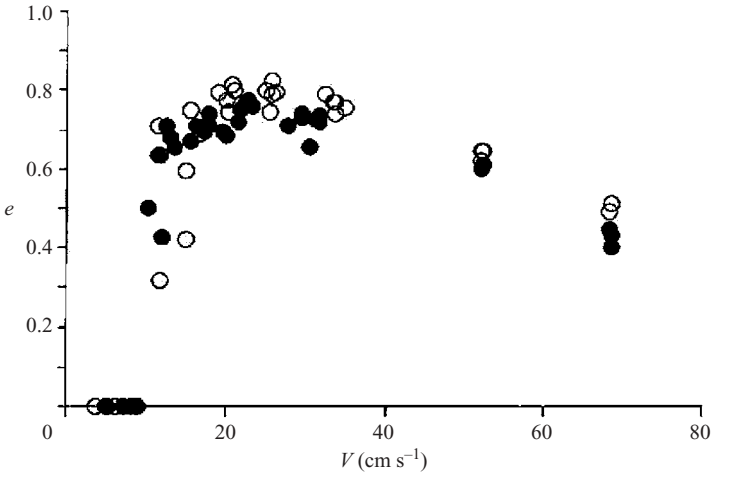


FIGURE 5. Restitution coefficient for millimetric water drops hitting a super-hydrophobic surface. As in figure 4, a loss of elasticity is observed with increasing the impact speed. Contrasting with Leidenfrost drops, the elasticity sharply decreases at small impact velocity, for which a sticking transition is observed. These data also emphasize that the drop behaviour is quite similar for water (open symbols) and a mixture of water and glycerol twice as viscous (solid symbols).

as large as 0.85 – a value significantly lower than reported for Leidenfrost drops in figure 4. This also suggests that the minimum velocity above which a rebound can be seen could be taken as a criterion of super-hydrophicity: the smaller this velocity, the better the surface – the limit being a hot plate for which this velocity appears to be zero.

## 4. Poorly elastic shocks

### 4.1. *Liquid springs*

As sketched in figure 6, we propose to model a bouncing drop as a spring. The simplest object which can be imagined for this purpose is a spring of initial length $l_0$ and stiffness $k$ with two masses $m/2$ attached at each end. The rebound can be divided in two phases: first, the drop spreads owing to its kinetic energy, so that it (partially) stores it as surface energy (as a compressed spring does as elastic energy); then, the drop transfers its surface energy to translational kinetic energy (allowing it to take off) and to oscillatory kinetic energy. Similarly, a compressed spring will oscillate as it takes off. We shall justify in the final discussion (§ 5.3) why usual sources of dissipation can be neglected in our model.

We now describe the spring case in more detail. Newton's equation of motion can be written for the two masses, whose positions are denoted $x_1$ (at the top of the drop) and $x_2$ (at the bottom):

$$\tfrac{1}{2}m\frac{\mathrm{d}^2x_1}{\mathrm{d}t^2} = -\tfrac{1}{2}mg - k(x_1 - x_2 - l_0) \tag{4}$$

for the first mass and:

$$\tfrac{1}{2}m\frac{\mathrm{d}^2x_2}{\mathrm{d}t^2} = -\tfrac{1}{2}mg - k(x_2 - x_1 + l_0) + F \tag{5}$$

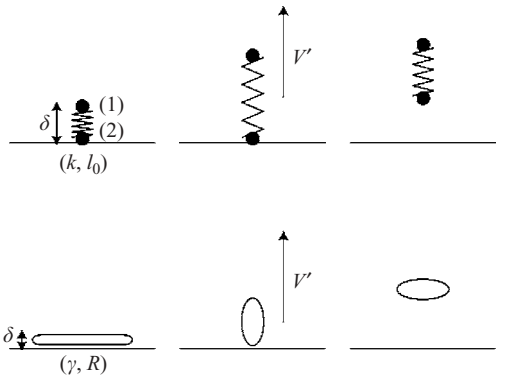


FIGURE 6. Comparison between a spring consisting of two attached masses, with an initial length $l_0$, a stiffness $k$ and compressed to a height $\delta$ and a bouncing drop of initial radius $R$, stiffness $\gamma$ and compressed to a height $\delta$.

for the second one, denoting the reaction of the solid $F$ (without adhesion, $F$ is positive). Initially, and as long as the force acting on mass 2 is negative (and balanced by $F$), we have $x_2 = 0$. Equation (4) can be integrated, taking as initial conditions an imposed compression $\delta$, and a zero velocity. Thus we find:

$$x_1(t) = l_0 - \frac{mg}{2k} + \left(\delta - l_0 + \frac{mg}{2k}\right)\cos\omega t \tag{6}$$

where $\omega$ is the natural pulsation of the mass:

$$\omega = \sqrt{\frac{2k}{m}}. \tag{7}$$

The bottom mass 2 leaves the substrate if the force which acts on it is positive ($k(x_1 - l_0) - mg/2 > 0$). Replacing $x_1$ by the quantity calculated above in (6), we find the time $t_o$ after which the mass takes off:

$$-mg + k\left(\delta - l_0 + \frac{mg}{2k}\right)\cos\omega t_o = 0. \tag{8}$$

This equation only admits a solution if the absolute value of $\cos\omega t_o$ is smaller than unity. Since also $\delta < l_0$, we finally find:

$$\delta < l_0 - \frac{mg}{k}. \tag{9}$$

The spring must be compressed enough to overcome its weight. If this criterion is fulfilled, we can calculate the speed at take off. Then $x_2(t_o) = 0$ and (from (6))

$$\frac{\mathrm{d}x_1}{\mathrm{d}t}(t_o) = -\omega\left(\delta - l_0 + \frac{mg}{2k}\right)\sin\omega t_o.$$

In the limit of a compressed spring ($\delta \ll l_0$), and denoting $x(t)$ as the position of the centre of mass of the spring, we find for the speed of take off:

$$V' = \frac{\mathrm{d}x}{\mathrm{d}t}(t_o) = \frac{\omega l_0}{2}\sqrt{\left(1 - \frac{g}{\omega^2 l_0}\right)\left(1 + \frac{3g}{\omega^2 l_0}\right)}. \tag{10}$$

If, in addition, the weight is negligible compared to the elastic energy typically stored in the spring ($mg \ll kl_0$), we simply find

$$V' = \frac{\omega l_0}{2} \tag{11}$$

These two limits ($\delta \ll l_0$ and $mg \ll kl_0$) are satisfied in our experiments: the size of the spring is the drop radius (or diameter); the compression due to impact is the drop thickness $\delta$ as it reaches its maximum extension (given by (3), which together with volume conservation yields $\delta \sim R\,We^{-1/2}$); and the stiffness of the spring is the surface tension $\gamma$. Thus these two conditions can be written for a bouncing drop as $We > 1$ and $R < \kappa^{-1}$, respectively, which are both fulfilled in this section. More generally, the results found for a spring should hold for a drop: the main difference between the two systems is the way the mass is distributed in space, which should affect the numerical coefficients but not the scaling laws. Equation (11) can be used for evaluating the speed after take off:

$$V' \sim V_o = \sqrt{\frac{\gamma}{\rho R}}. \tag{12}$$

This is quite a surprising result: the speed of take off $V'$ is independent of the impact speed $V$ (for $We > 1$, i.e. in the regime of large deformation), so that the restitution coefficient $e = V'/V$ should decrease with $V$, as

$$e \sim We^{-1/2}. \tag{13}$$

This result is in good agreement with the results displayed in figures 4 and 5. This shows *a contrario* that the speed after take off is the same whatever the impact speed. For a millimetric drop, this speed is about $25\,\mathrm{cm\,s^{-1}}$, in agreement with the value deduced from (12). With such a speed, the drop rises to a height of about 3.5 mm (as can be observed in figure 1). Since $V'$ does not depend on the compression of the drop, the details of the model providing the rate of compression ((2) or (3), for example) do not have an impact on the result. This also helps in understanding the difference between these kinds of shock and shocks of solid marbles. In the latter case, the impact object mainly deforms close to its contact with the solid on which it bounces, and it stores its kinetic energy as (volumetric) elastic energy. Then, the restitution coefficient increases with the speed $V$ at impact, before saturating (and very slightly decreasing) at very large $V$ (Falcon *et al.* 1998). It seems that the energy transferred (and later lost) to vibrational modes is negligible, compared to the energy dissipated in elastic waves at the substrate surface and in plastic deformation in the impacting body.

### 4.2. *Conditions for a rebound*

The mass–spring analogy also helps in understanding the criterion for observing a rebound. We stressed earlier that the elastic force must overcome the weight to allow take off, (9). In our case, the compression is the height of the drop after it has been squeezed by the impact: the drop is more compressed when the impact is violent (figure 3). Thus, we expect from (9) that a rebound can only occur provided that the speed is large enough. For $We > 1$, (3) can be considered as a law for the compression; using volume conservation, it yields $\delta \sim R\,We^{-1/2}$. Then, replacing the different terms in (9) (i.e. taking $l_0 \sim R, k \sim \gamma$ and $m \sim \rho R^3$) yields as a criterion of bouncing:

$$V > V_c = \frac{V_o}{(1 - R^2\kappa^2)} \tag{14}$$

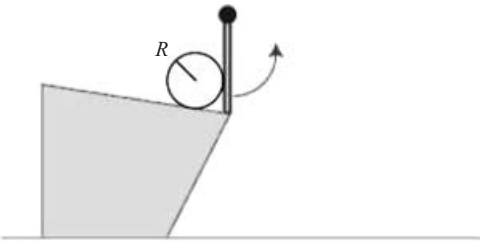


FIGURE 7. Our device for varying the size of the bouncing drop: a volume of water (radius $R$) is deposited on a slightly inclined plate. When the gate is opened, the drop falls and bounces on the plate below. All the elements are made of steel and heated, so that the drop is everywhere in a Leidenfrost situation.

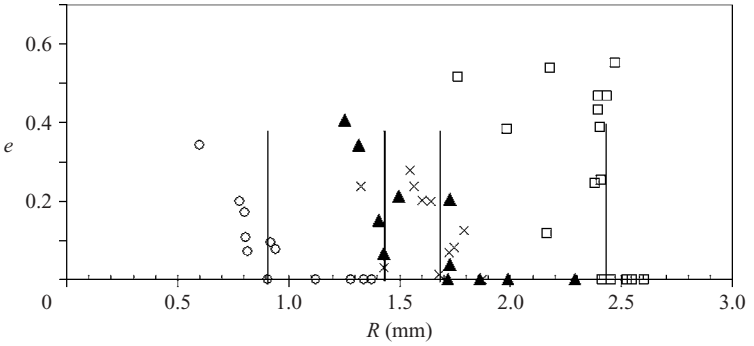


FIGURE 8. Restitution coefficient of the shock for a drop of varying radius $R$ falling from a given height $H = 1$ cm, as a function of $R$ for different liquids (○, liquid nitrogen; ▲, ethanol; ×, acetone; □, water). In each case, an abrupt decrease is observed around a critical radius $R_c$ marked with a vertical line.

where $V_o$ is defined by (12), and is about 25 cm s$^{-1}$ for a millimetric water drop. For small droplets ($R \ll \kappa^{-1}$), (14) indicates that drops will only bounce if $V > V_o$, that is, $We > 1$, which is the limit considered in this section. But it can be different if drops are larger: as $R$ approaches the capillary length $\kappa^{-1}$, the velocity $V_c$ diverges, meaning that drops which satisfy the condition $We > 1$ will not necessarily bounce. Note that this result does not depend on the choice of the model for spreading: using (2) for evaluating the compression of the drop leads to a relation similar to (14), but with a different diverging behavior as $R$ approaches $\kappa^{-1}$ (then, we find $V > V_c = V_o/(1 - R^2\kappa^2)^2$).

To test these ideas, we performed the experiment sketched in figure 7. A steel block with a slightly inclined (by 1° or 2°) top plate is heated above the Leidenfrost temperature $T_L$. Liquids are kept trapped on the top plate by a steel gate, which is similarly brought above $T_L$. When the gate is opened, the drop falls down till it reaches another flat plate also above $T_L$. Movies of the fall and the (possible) rebound were made for different liquids (water, ethanol, acetone and liquid nitrogen). In each case, the size of the initial drop was varied, and the velocity of impact kept as constant as possible, between 42 and 51 cm s$^{-1}$. This variation together with the uncertainty in the measurement of $V'$ generate some scatter in the results displayed in figure 8, where the restitution coefficient $e$ is plotted as a function of the drop radius.

For each liquid, it is observed that $e$ dramatically decreases when approaching some critical size $R_c$ of the drop. This size is quite comparable for ethanol and acetone, but

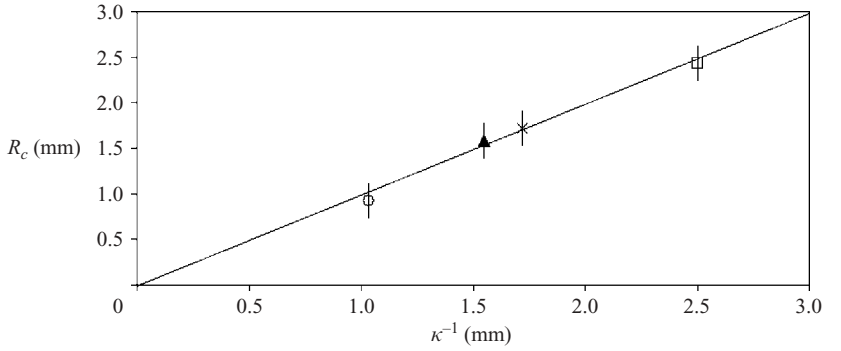


FIGURE 9. Critical radius $R_c$ above which a Leidenfrost drop does not bounce, as a function of the capillary length associated with the liquid (○, liquid nitrogen; ▲, ethanol; ×, acetone; □, water), as deduced from figure 8.

significantly smaller for liquid nitrogen, and larger for water. For drops larger than $R_c$, the shock is inelastic ($e = 0$): a 'large' drop cannot bounce, despite the (quasi-) absence of friction for these non-wetting systems.

We plot in figure 9 the critical radius $R_c$ as a function of the capillary length. It is observed that the two quantities are proportional to each other, with a constant of proportionality close to unity ($R_c\kappa = 1.0 \pm 0.1$). This result agrees with (14), which predicts that bouncing should not occur (whatever the impact velocity) for drops of the order of (or larger than) $\kappa^{-1}$. This result can be summarized in a very simple way: a drop larger than the capillary length is subject to gravity, which makes it flatten. Thus, such a drop loses its elasticity, which makes it unable to bounce. Such large drops were observed to just oscillate on the plate, after hitting it; these oscillations were damped by viscosity, yet sometimes reappeared spontaneously, as reported by Yoshiyasu, Matsuda & Takaki (1996) or by Strier *et al.* (2000). More generally, the loss of elasticity could arise from other factors, such as viscosity or adhesion. However, transitions to sticking in these cases remain to be described.

## 5. Quasi-elastic shocks

### 5.1. *Phenomenology*

It was observed in figure 4 that a rebound at a small Weber number is characterized by a very high restitution coefficient. Let us first stress that such impacts are difficult to achieve: $We \ll 1$ implies for a millimetric drop an impact velocity smaller than $25\,\mathrm{cm\,s^{-1}}$, corresponding to a drop released from a height smaller than 3 mm. Thus we chose to study series of rebounds: a given drop is released from a centimetric height, and its successive rebounds are monitored as a function of time. This allows us to reach (after a few rebounds, and provided that the substrate is exactly horizontal) impact velocities of the order of $0.1\,\mathrm{m\,s^{-1}}$, or even smaller. However, this does not avoid the vibrations of the drop (which oscillates after each rebound, as described in § 2), which will be found to affect the rebound.

Figure 10 shows the restitution coefficient of a water drop bouncing off hot plates, as a function of the number of rebounds. Very numerous rebounds are observed: for similar experiments, we monitored up to 1000 successive rebounds, which emphasizes the quasi-elasticity of the shocks. In figure 10, the restitution coefficient is indeed observed to tend after about 10 shocks towards a value which is very close to

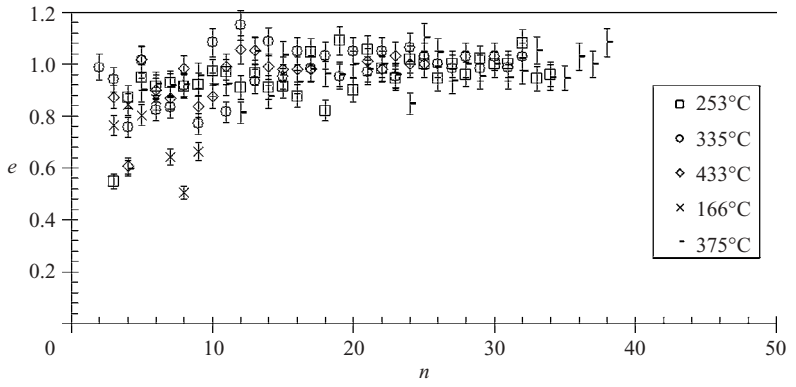


FIGURE 10. Restitution coefficients observed for series of successive rebounds experienced by water drops falling from an initial height of 16 mm; $n$ designates the number of rebounds. Whatever the plate temperature, the restitution coefficient tends towards a value very close to unity (quasi-elastic regime), allowing a very large number of successive rebounds (here tens, but we often observed hundreds).

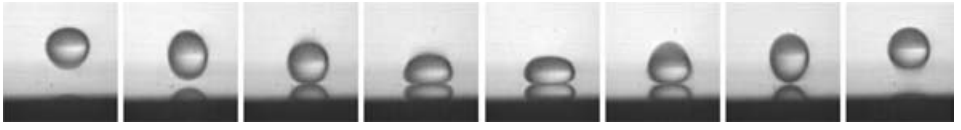

FIGURE 11. Sequence of pictures showing the rebound of a water Leidenfrost drop in the quasi-elastic regime. The drop radius is $R = 1$ mm, the impact velocity is $V = 7\,\mathrm{cm\,s^{-1}}$, which yields a Weber number $We = 0.1$. The interval between two pictures is 2.5 ms.

unity, whatever the plate temperature (provided it is larger than the Leidenfrost temperature). Hence the drop always rises to the same height (independent of the position from which it is released), which is of the order of 2 mm for a drop of radius $R = 1$ mm. Note also in figure 10 that the restitution coefficient can be larger than unity; this is partially related to the uncertainty in the measurement, but values larger than 1 might indeed exist, because of the oscillations of the drop (which store some energy), and possibly because of the energy gained on the hot plate (close to which the drop slightly evaporates).

Figure 11 shows the successive positions of a drop in one period of this stationary elastic regime. The drop deforms modestly during the contact ($We \ll 1$). Its size remains constant during the period, showing that evaporation can be neglected at this time scale (this allows the drop to bounce several hundreds times). The period in figure 11 is $17.5 \pm 1.0$ ms, a time negligible compared to the lifetime of this Leidenfrost drop, if deposited (and trapped) on the hot plate, namely 40 s (at 250 °C). (This lifetime is observed to remain of the same order for a bouncing drop.) But most importantly, it can be seen in figure 11 that the vibrations of the drop coincide with its rebound: the drop is spherical at impact and take off; it flattens twice, namely during the contact and when it reaches its maximum height. It thus seems that the oscillations are synchronized with the motion of the centre of mass.

We recorded the mean height of the drop $h$ (that is, the position of its centre of mass) together with its equatorial diameter $d$, as a function of time, for several successive oscillations (and rebounds). Figure 12($a$) shows that both curves are periodic, without significant damping, and that the period is indeed the same. For a better visualization,

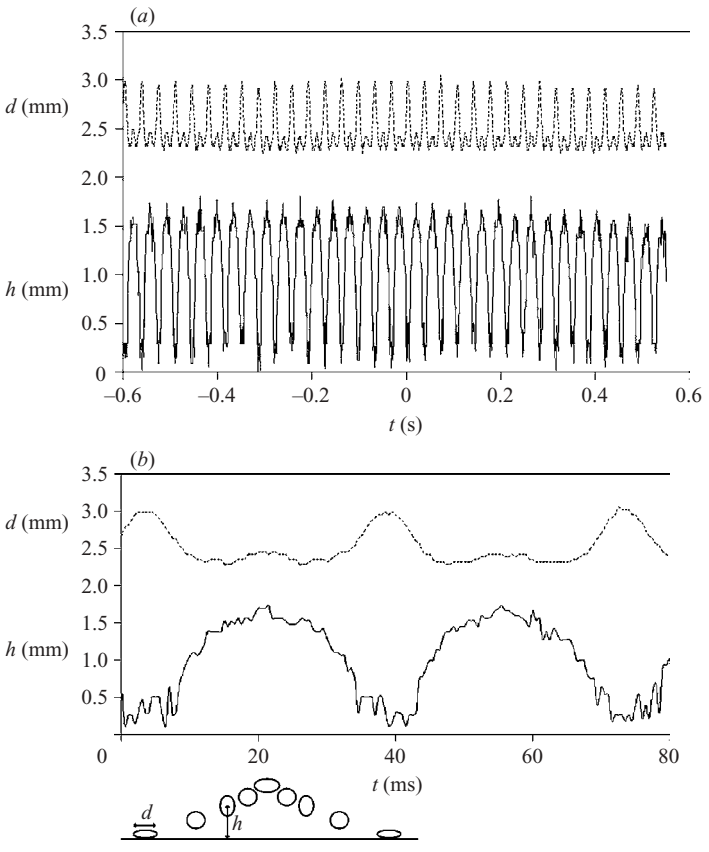


FIGURE 12. (*a*) Height $h$ of the centre of mass of a water drop ($R = 1.25$ mm) in the quasi-elastic regime: no appreciable decrease of the height is observed over more than 30 successive rebounds. We show in the same plot the equatorial diameter $d$ of the drop: the vibrations generated by the impact (and seen in figure 11) are observed to be in phase with the flight. (*b*) Zoom of two periods of (*a*). We sketch below the shape at the drop for different moments of its flight.

figure 12(*b*) is a zoom of two periods, together with a sketch of the successive shapes of the drop within a period. The drop undergoes half an oscillation on the plate, and one and a half in air. The respective durations of these two regimes are 10 ms and 25 ms, from which we deduce that the period of oscillation is different when the drop is contacting the solid (then, the period is 20 ms) and when it is free (then, the period is 16.7 ms), as mentioned in Courty *et al.* (2006).

Taking the flight time to be of the order of the oscillation time, we can deduce a simple formula for the height of the drop $h_c$ in the regime of multiple rebounds. Taking the Rayleigh time $\pi(\rho R^3/2\gamma)^{1/2}$ of oscillation of a free drop (Rayleigh 1879), and that the time of the flight $t$ (related to the height by $h = gt^2/8$) is 1.5 the oscillation time of a drop, we find a relation between $h_c$ and the drop radius:

$$h_c = \frac{9\pi^2}{64}\frac{R^3}{\kappa^{-2}}. \tag{15}$$

We tested this relation, and plot our results in figure 13. The domain of variation is quite limited for the drop radius. On the one hand, we are limited by the capillary

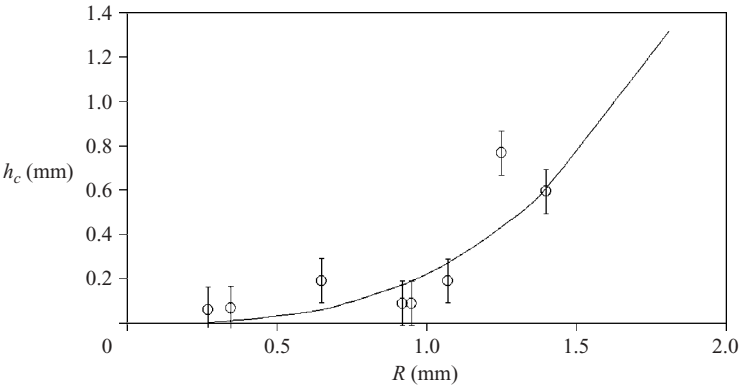


FIGURE 13. Height for which multiple rebounds are observed as a function of the drop radius. The data are compared with (15), drawn as a line.

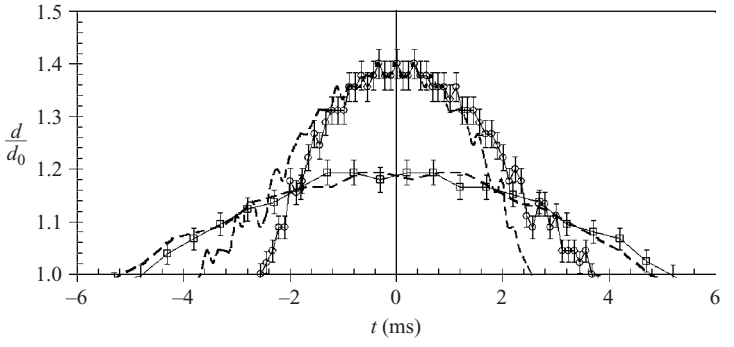


FIGURE 14. Equatorial diameter of an impacting drop (normalized by its diameter before impact) as a function of time, for a drop in the quasi-elastic regime (squares) and for a drop for which the oscillation and flight periods differ (circles). The origin of time is chosen at the maximal extension. It is observed that only the drop deformation is time-reversible, in the quasi-elastic regime only.

length $\kappa^{-1}$, as shown in §4.2. On the other hand, the drop cannot be smaller than a fraction of a millimetre for the observation to be feasible. On the whole, a fair agreement is found, without any adjustable parameter.

### 5.2. *Conditions for observing a quasi-elastic rebound*

We tried to characterize the conditions which favour a quasi-elastic rebound. We first compared shocks for which the restitution coefficient $e$ could not be distinguished from unity with shocks for which it was found to be significantly smaller. We display in figure 14 an interesting difference between the two cases: the drop diameter (normalized by its value without oscillation) is plotted as a function of time during the shock: it thus in both cases increases from unity to a value slightly larger (1.2 and 1.4), before decreasing back to unity (when the drop takes off). The origin of time is chosen as the maximum extension. For each series of data (symbols), we superimposed (thin lines) curves and they are time-symmetric. It is found that only the quasi-elastic rebound (squares) is time-reversible, which stresses the phase locking between the two sources of oscillation (drop vibration, parabolic flight).

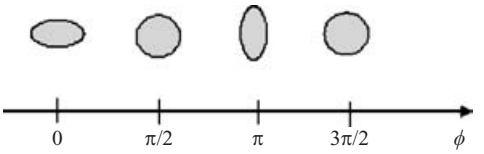


FIGURE 15. Our phase convention for a drop subjected to a quadrupolar oscillation.

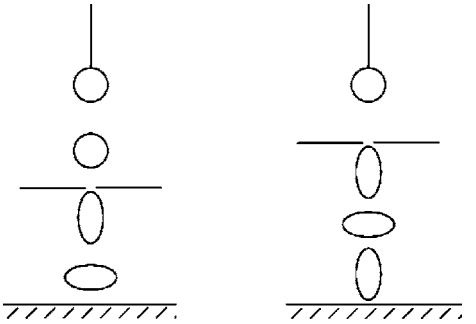

FIGURE 16. Experimental set-up for tuning the phase of a drop at impact. A plate pierced with a hole of millimetric diameter (and heated to be non-wettable) is placed between the height from which the liquid is released and the bottom plate on which the rebound is observed. Passing through the hole elongates the drop, which later oscillates. Varying the position of the pierced plate thus allows us to vary the phase at impact.

A natural question, at this point, is how elastic (or less elastic, as shown in figure 4) regimes may be generated. We noted above (figure 10) that the elastic regime spontaneously sets in after a short transient. It happens in about 70 % of the experiments where we followed successive rebounds, and always exhibits the characteristics reported above (synchronization of the oscillation with the flight, time-reversibility). This suggests that the phase of the drop influences the rebound, and we thus tried to demonstrate the role of this phase.

We chose for the phase of the drop oscillation the convention sketched in figure 15. Note that the two spherical states ($\phi = \pi/2$ and $\phi = 3\pi/2$) differ by the internal motion of the liquid: the equatorial diameter tends to contract in the phase $\phi = \pi/2$, while it tends to expand in the phase $\phi = 3\pi/2$. Our experiment consisted of monitoring impacts for similar drops having a similar velocity, yet a different phase at impact. The phase was varied using the device drawn in figure 16: a plate pierced with a thin hole (diameter comparable with that of the drop) is placed between the point from which the drop is released and the plate. Because of the presence of this hole, the drop is forced to elongate (and then vibrates), so that changing the height of the pierced plate allowed us to vary the phase at impact. The impact was recorded and the restitution coefficient of the shock deduced from the record.

Despite its apparent simplicity, this experiment is extremely delicate to perform at very small impact velocities (where the elastic regime is observed), because this corresponds to small heights, which makes it impossible to place the pierced plate. We thus were forced to do this experiment with various heights (of the order of one centimetre), corresponding to impact velocities between 20 and 80 $\mathrm{cm\,s^{-1}}$. We carefully measured the restitution coefficients for about 100 shocks in this interval of impact velocities, allowing us to determine a mean value $\bar{e}$ of $e$ for each velocity. The results are displayed in figure 17, where for each shock we normalized the measured

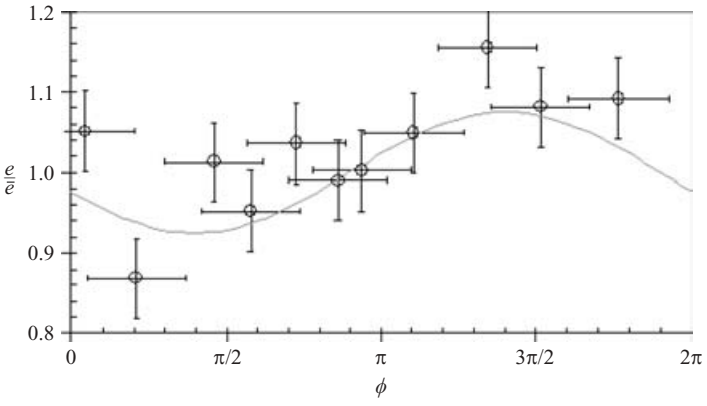


FIGURE 17. Restitution coefficient of a drop bouncing off a hot plate as a function of its phase at impact (defined in figure 15). The restitution coefficient is normalized by its mean value at a given impact velocity. Each datum corresponds to at least five experiments, and the corresponding error bars are indicated.

restitution coefficient by its mean value at this velocity. This explains why in our results the quantity $e/\bar{e}$ can be larger than unity. The uncertainty in the determination of the phase at impact is 0.3 rad. We performed (on average) 5 measurements per interval of 0.3 rad, which provides the uncertainty in the coefficient of restitution.

It appears that the phase does affect the elasticity of the shock: the data can be fitted by a sinusoidal function, whose maximum is observed for $\phi = 1.4\pi$, close to $3\pi/2$. The effect is small, yet significant: the relative increase in measured restitution coefficient between $\phi = \pi/2$ and $3\pi/2$ is about 40 %, larger than the uncertainty on the measurement ($\pm 10$ %). The maximum elasticity is found to be reached for the phase ($\phi = 3\pi/2$) observed for impacting drops in the quasi-elastic regime. The system thus locks onto the state of minimum dissipation. By definition, the phase $\phi = 3\pi/2$ is the one for which the drop is spherical, coming back from an oblate configuration. In the reference frame of the drop, the velocity of the bottom of the drop is directed towards the top, and it is maximum in this phase. Since the drop is moving at a velocity $V$, this phase thus corresponds to the minimum velocity of the bottom of the drop. On the other hand, the phase $\phi = \pi/2$ has a maximal velocity, and was observed to be the less elastic. It seems that the local velocity at impact might influence the elasticity, which is advantageous since this velocity is small.

We can evaluate this minimal velocity. In the regime of small deformation, we assume that there is energy conservation (Okumura *et al.* 2003): at impact, the drop stores its kinetic energy as surface energy. Denoting as $\varepsilon_o$ the increase of radius in the oblate state ($\phi = \pi$, see figure 15), the conservation of energy is written dimensionally as $\rho R^3 V^2 \sim \gamma \varepsilon_o^2$, which gives $\varepsilon_o$ ($\varepsilon_o \sim RWe^{1/2}$). The elongation of the drop radius can be written $\varepsilon = \varepsilon_o \sin(\omega t - 3\pi/2)$, where $\omega$ is the Rayleigh pulsation of a free drop ($\omega \sim (\gamma/\rho R^3)^{1/2}$). As the drop impacts, the bottom moves up at a velocity $\varepsilon_o \omega$, that is, of the order of $V$, the impact velocity of the centre of mass. Hence, the drop touches the solid with a minimized velocity, which accounts for a minimized energy loss during the shock.

### 5.3. *Discussion*

Periodic rebounds are also observed for solid marbles bouncing off vibrated plates. Depending on the pulsation $\omega$ and amplitude $A$ of the vibrations, the marble may

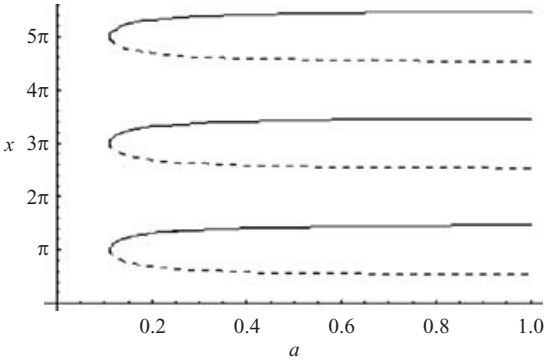


FIGURE 18. Numerical solution of (20), as a function of the amplitude of the oscillation. For the resolution, we have chosen $R = 1.1$ mm and $e_o = 0.9$. For each family of solution, there is one stable branch (solid line), and one unstable branch (dashed line).

bounce, or not. Also, there is a correlation between the time of flight and the period of vibration. In our case, we must first write an equation for the shock – as discussed above, the restitution coefficient varies with the phase, and with the impact velocity: $e = e_o\ (1 - kA/R\ \sin\phi)\ (b + cV)$, where $A$ is the amplitude of the oscillation and $b$, $c$ and $\beta$ are coefficients. Neglecting the variation of the restitution coefficient with the velocity (which yields a second-order correction), we obtain a relationship between the take-off and impact velocities:

$$V' = Ve_o(1 - \beta A/R \sin\phi). \tag{16}$$

The phase at take-off is $\pi/2$. Denoting the time of flight (between two impacts) as $\tau$, we thus find for the phase at impact:

$$\phi = \omega\tau + \frac{\pi}{2}. \tag{17}$$

When in the air, the drop is subject only to gravity; in the quasi-elastic regime, it falls towards the plate at the same velocity $V$ as for the previous shock, which is written

$$V = V' - g\tau. \tag{18}$$

Since the trajectory of the bottom of the drop $z_b$ is $z_b = -gt^2/2 + V't + A\cos(\omega t + \pi/2)$, we obtain a third equation at contact:

$$-\tfrac{1}{2}g\tau^2 + V'\tau - A\sin\omega\tau = 0. \tag{19}$$

Denoting $x = \omega\tau$ and $a = A/R$, the solution of these equations satisfies

$$(1 - e_o)\frac{x^3R^2\kappa^2}{16} + \frac{e_o}{2}a\sin 2x + e_o\frac{R^2\kappa^2}{16}\beta x^2\cos x + (1 - e_o)\sin x = 0 \tag{20}$$

where $\kappa$ is the inverse of the capillary length. Equation (20) can be solved numerically ($x$ being the unknown), which was done for $\beta = 1$ (the solutions depend little on the value of this parameter). The solutions are displayed in figure 18, as a function of $a$, the reduced amplitude of the oscillation, for a water drop at 100 °C of radius $R = 1.1$ mm and for $e_o = 0.9$.

It is observed that periodic solutions exist provided that the amplitude of the oscillation is larger than a threshold $a_c = (1 - e_o)/e_o$, i.e. about 0.1 in the example of figure 18. These solutions tend towards $\pi$, $3\pi$, $5\pi$ at small amplitude, which seems in

good agreement with our experimental results: the periodic regime described above corresponds to $x = 3\pi$, and we observed drops oscillating twice during the flight, corresponding to $x = 5\pi$. A different choice for $\beta$ would slightly shift the threshold amplitude $a_c$. Note also that only half of the branches are stable in figure 18, as indicated (the stability is deduced from the evolution of the trajectory after perturbing the time of flight). It is thus possible to observe periodic regimes – and, as found experimentally, this might be not the case, which is found to be due to an too small amplitude. For most observations, the amplitude was found to be about $0.15R$, in qualitative agreement with the results in figure 18. Because of the modest value of this amplitude, $x$ should be close to its minimal value of $3\pi$, as indeed found in the experiments.

We assumed in this description that the amplitude of the oscillation remains constant throughout the sequence, which was observed experimentally. This raises the question of dissipation and energy input in these processes, which we discuss finally.

The oscillations might be damped principally by viscosity. The typical time associated with this damping scales as $\rho R^2/\eta$, and is found to be about 3 s for a millimetric drop of water (whose viscosity falls to about 0.3 mPa s at 100 °C). It is much longer than a typical time of flight (i.e. a few milliseconds), allowing us to understand the negligible role of the liquid viscosity in these experiments.

Conversely, the drop can gain momentum during the impact because of its evaporation (by a quantity $\delta m$), which might sustain the rebounds. The corresponding gain of energy scales as $\delta m V^2$. Denoting as $\tau$ the contact time of the drop (see figure 2), and $\tau_L$ as its lifetime, we expect $\delta m$ to be of the order of $m\tau/\tau_L$; for $\tau = 10$ ms, $\tau_L = 40$ s and $R = 1$ mm, we find $\delta m$ of about $10^{-9}$ kg. On the other hand, the loss of translational kinetic energy due to impact can be written $mV^2(1 - e^2)$. Taking $e$ of about 0.9, that is, a typical value observed on a cold super-hydrophobic surface in the regime of high elasticity, the ratio between these two energies scales as $\delta m/m(1 - e^2)$. This is typically $10^{-3}$, suggesting that the main cause of elasticity, in this system, is the absence of pinning on the hot solid, rather than drop evaporation. The elasticity could also be reduced by the presence of the vapour film, which was treated in the paper as a passive medium allowing a non-wetting situation. The viscous force associated with the spreading of the drop (roughly) scales as $\eta_a V/h_f R_M^2$ (with $\eta_a$ and $h_f$ the vapour film viscosity and thickness), and thus the energy dissipated by viscosity as $\eta_a V/h_f R_M^3$. For large Weber numbers, equation (3) gives $R_M$ ($R_M \sim R\,We^{1/4}$). We can thus compare the energy lost by viscosity to the kinetic energy of the impinging drop, which is written $\eta_a/\rho V h_f\ We^{3/4}$. For standard values of the different parameters (in particular taking $h_f$ of the order of 100 μm), we find a value of about $10^{-4}$ for the first dimensionless group $\eta_a/\rho V h_f$, which implies a negligible viscous loss (in the vapour film) during the spreading stage. This partially justifies why we could ignore dissipation in our spring model.

## 6. Conclusion

We report in this paper a series of experiments showing the rebounds of liquid droplets of low viscosity hitting very hot plates, in the so-called Leidenfrost situation – a question of practical importance in cooling and deposition processes. We focused on the elasticity of the shock, and found that two regimes of bouncing can be distinguished, depending on the Weber number.

When the inertia of the falling droplet is large compared to its surface tension (high Weber number), the rebound is less elastic since the impact speed is large.

This considerably differs from solid elastic shocks at similar velocities, for which the elasticity only weakly depends on the impact velocity. This difference is related to the loss of energy associated with the shock in a liquid, which has two main causes: dissipation during the spreading at the impact, and partition of the energy between drop oscillations and translation at take-off. The higher the velocity, the larger the part of energy which is transferred to oscillations, and thus the less elastic the shock. In a similar vein, it is found that elasticity will be lost for large drops: then, the impact is found to be inelastic; owing to gravity, drops larger than the capillary length cannot restore enough translational energy to take off, and thus remain stuck on the hot plate where they oscillate without bouncing.

For shocks at a small Weber number, we report the existence of a quasi-elastic regime of rebounds: a drop may bounce hundreds of times, always coming back to the same (millimetric) height. Then, it is observed that there is a strong correlation between the oscillations of the drop and the rebound: the sequence of oscillations exactly fits with the drop trajectory, so that time reversibility is obeyed. The effect of the drop oscillations at the first impact is experimentally addressed, and results suggest that a bouncing drop maximizes its elasticity by adjusting its flying time to its oscillations. A successively bouncing drop reaches a resonant state where the energy loss is minimized.

As has been mentioned in the past, the bouncing of a drop is very similar to its oscillation. In this respect, one can not the strong similarity between the behaviour of a drop on an oscillating plate and a Leidenfrost drop (Yoshiyasu *et al.* 1996). If the frequency and the amplitude are in the correct range, a small drop on a non-wetting oscillating plate bounces periodically. If the size of the drop is increased (puddles), the drop remains stuck to the plate because of gravity (as for large Leidenfrost drop impact) and oscillates, displaying star shapes (spontaneously oscillating Leidenfrost stars may also be observed (Strani & Sabetta 1983; Strier *et al.* 2000)). We proposed in some (favourable) cases qualitative explanations for the observed phenomena, but many questions remain, often related to energy conservation (or loss) in these systems: it might be worth describing how viscosity modifies our picture. It would also be useful to understand if the quasi-elastic regime is specific to the Leidenfrost situation: would a drop in zero-wetting bounce similarly on a cold solid (i.e. without any evaporation)? Owing to residual adhesion, it would be very difficult to answer this question experimentally. Numerical simulations, well-adapted to these slippery states of water where the absence of any contact lines simplifies the approach (Renardy *et al.* 2003) might be very useful. They would also contribute to showing how the frequency locking is found by the system. The same kind of approach would be very useful to confirm and make more quantitative our observation on the dependence of the restitution coefficient on the oscillation phase of the impacting drop.

## REFERENCES

Baumeister, K. J. & Simon, F. F. 1973 Leidenfrost temperature – its correlation for liquid metals, cryogens, hydrocarbons, and water. *Trans. ASME: J. Heat Transfer* **95**, 166–173.

Bell, K. J. 1967 The Leidenfrost phenomenon: a survey. *Chem. Engng Prog. Symp. Series AIChE* **63**, 351–358.

Berenson, P. J. 1961 Film-boiling heat transfer from a horizontal surface. *Trans. ASME: J. Heat Transfer* **83**, 351–358.

Biance, A. L., Clanet C. & Quere, D. 2003 Leidenfrost drops. *Phys. Fluids* **15**, 1632–1637.

Chandra, S. & Avedisian, C. T. 1991 On the collision of a droplet with a solid surface. *Proc. R. Soc. Lond.* A **432**, 13–41.

Chandra, S. & Aziz, S. D. 1994 Leidenfrost evaporation of liquid nitrogen droplets. *Trans. ASME: J. Heat Transfer* **116**, 999–1006.

Clanet, C., Béguin, C., Richard, D. & Quéré, D. 2004 Maximal deformation of an impacting drop. *J. Fluid Mech.* **517**, 199–208.

Courty, S., Lagubeau, G. & Tixier, T. 2006 Oscillating droplets by decomposition on the spherical harmonic basis. *Phys. Rev.* E (in press).

Eggers, J., Lister, J. & Stone, H. A. 1999 Coalescence of liquid drops. *J. Fluid Mech.* **401**, 293–310.

Falcon, E., Laroche, C., Fauve, S. & Coste, C. 1998 Behaviour of one inelastic ball bouncing repeatedly off the ground. *Eur. Phys. J.* B **3**, 45–57.

Goldshtik, M., Khanin, V. & Ligai, V. 1985 A liquid drop on an air cushion as an analogue of Leidenfrost boiling. *J. Fluid Mech.* **166**, 1–20.

Gottfried, B. S., Lee, C. J. & Bell, K. J. 1966 The Leidenfrost phenomenon: film boiling of liquid droplets on a flat plate. *Intl J. Heat Mass Transfer* **9**, 1167–1187.

Karl, A. & Frohn, A. 2000 Experimental investigation of interaction processes between droplets and hot walls. *Phys. Fluids* **12**, 785–796.

Leidenfrost, J. G. 1756 *De Aquae Communis Nonnullis Qualitatibus Tractatus.* Duisburg.

Michiyoshi, I. & Makino, K. 1978 Heat transfer characteristics of evaporation of a liquid droplet on heated surface. *Intl J. Heat Mass Transfer* **21**, 605–613.

Okumura, K., Chevy, F., Richard, D., Quéré, D. & Clanet, C. 2003 Water spring: a model for bouncing drops. *Europhys. Lett.* **62**, 237–243.

Rayleigh, Lord 1879 On the capillary phenomena of jets. *Proc. R. Soc. Lond.* **29**, 71–97.

Rein, M. 1993 Phenomena of liquid drop impact on solid and liquid surfaces. *Fluid Dyn. Res.* **12**, 61–93.

Renardy, Y., Popinet, S., Duchemin, L. *et al.* 2003 Pyramidal and toroidal water drops after impact. *J. Fluid Mech.* **484**, 69–83.

Richard, D. 2000 Situations de mouillage nul. PhD Thesis, University of Paris VI.

Richard, D., Clanet, C. & Quéré, D. 2002 Contact time of a bouncing drop. *Nature* **417**, 811.

Richard, D. & Quéré, D. 2000 Bouncing water drops. *Europhys. Lett.* **50**, 769.

Strani, M. & Sabetta, F. 1983 Free vibrations of a drop in partial contact with a solid support. *J. Fluid Mech.* **141**, 233–247.

Strier, D. E., Duarte, A. A., Ferrari, H. & Mindlin, G. B. 2000 Nitrogen stars: morphogenesis of a liquid drop. *Physica* A **283**, 261–266.

Wachters, L. H. J., Bonne, H. & van Nouhuis, H. J. 1966 The heat transfer from a hot horizontal plate to sessile water drops in the spheroidal state. *Chem. Engng Sci.* **21**, 923–936.

Yoshiyasu, N., Matsuda, K. & Takaki, R. 1996 Self-induced vibration of a water drop placed on an oscillating plate. *J. Phys. Soc. Japan* **65**, 2068–2071.

Zhang, S. & Gogos, G. 1991 Film evaporation of a spherical droplet over a hot surface: fluid mechanics and heat/mass transfer. *J. Fluid Mech.* **222**, 543–563.